Original Article

MOLECULAR METABOLISM

Epidermal Acyl-CoA-binding protein is indispensable for systemic energy homeostasis

Ditte Neess [1,4], Vibeke Kruse [1,4], Ann-Britt Marcher [1], Mie Rye Wæde [1], Julie Vistisen [1], Pauline M. Møller [1], Rikke Petersen [1], Jonathan R. Brewer [1], Tao Ma [2], Georgia Colleluori [3], Ilenia Severi [3], Saverio Cinti [3], Zach Gerhart-Hines [2], Susanne Mandrup [1,*], Nils J. Færgeman [1,]**

ABSTRACT

Objectives: The skin is the largest sensory organ of the human body and plays a fundamental role in regulating body temperature. However, adaptive alterations in skin functions and morphology have only vaguely been associated with physiological responses to cold stress or sensation of ambient temperatures. We previously found that loss of acyl-CoA-binding protein (ACBP) in keratinocytes upregulates lipolysis in white adipose tissue and alters hepatic lipid metabolism, suggesting a link between epidermal barrier functions and systemic energy metabolism.
Methods: To assess the physiological responses to loss of ACBP in keratinocytes in detail, we used full-body ACBP$^{-/-}$ and skin-specific ACBP$^{-/-}$ knockout mice to clarify how loss of ACBP affects 1) energy expenditure by indirect calorimetry, 2) response to high-fat feeding and a high oral glucose load, and 3) expression of brown-selective gene programs by quantitative PCR in inguinal WAT (iWAT). To further elucidate the role of the epidermal barrier in systemic energy metabolism, we included mice with defects in skin structural proteins (*ma/ma Flg$^{ft/ft}$*) in these studies.
Results: We show that the ACBP$^{-/-}$ mice and skin-specific ACBP$^{-/-}$ knockout mice exhibited increased energy expenditure, increased food intake, browning of the iWAT, and resistance to diet-induced obesity. The metabolic phenotype, including browning of the iWAT, was reversed by housing the mice at thermoneutrality (30 °C) or pharmacological β-adrenergic blocking. Interestingly, these findings were phenocopied in flaky tail mice (*ma/ma Flg$^{ft/ft}$*). Taken together, we demonstrate that a compromised epidermal barrier induces a β-adrenergic response that increases energy expenditure and browning of the white adipose tissue to maintain a normal body temperature.
Conclusions: Our findings show that the epidermal barrier plays a key role in maintaining systemic metabolic homeostasis. Thus, regulation of epidermal barrier functions warrants further attention to understand the regulation of systemic metabolism in further detail.

Keywords Epidermal barrier; Energy expenditure; Adipose tissue; Browning; Diet induced obesity; β-adrenergic signaling; Acyl-CoA binding protein; Filaggrin

1. INTRODUCTION

The skin is the largest sensory organ of the human body, accounting for approximately 16% of total body weight. The skin barrier not only protects us from environmental xenobiotics, oxidative stress, and infections from various pathogens, but also regulates the amount of heat and water released from the body and senses various environmental changes including thermal variations [1]. Mammalian skin is comprised of three layers: the hypodermis, dermis, and epidermis. The epidermis is further subdivided into multiple layers, among which the outermost layer, the stratum corneum, provides an epidermal permeability barrier. It consists of terminally differentiated keratinocytes that are embedded in a highly ordered extracellular lipid-containing matrix. Numerous factors, including structural and junctional proteins, serve fundamental roles in the generation and maintenance of the epidermal permeability barrier including terminal epithelial differentiation products such as filaggrin, loricrin, certain keratins, and tight junctions. Lipids such as ceramides, sterols, and fatty acids are also crucial constituents of the epidermal barrier [2,3]. Accordingly, lipid metabolism serves fundamental roles in the generation and maintenance of the epidermal permeability barrier and proper insulation [2]. Functional loss of enzymes and transport proteins involved in lipid metabolism can result in severe desiccation and neonatal or premature death. However, non-lethal phenotypes including tousled and greasy fur, increased trans-epidermal water loss (TEWL), and alopecia have also been observed, for example in mice lacking stearoyl-CoA desaturase 1 (SCD1) [4], very long-chain fatty acid elongase 3 (ELOVL3$^{-/-}$) [5,6], or the alkaline ceramidase

[1]Department of Biochemistry and Molecular Biology, Villum Center for Bioanalytical Sciences, University of Southern Denmark, Campusvej 55, 5230, Odense M, Denmark [2]Novo Nordisk Foundation Center for Basic Metabolic Research, University of Copenhagen, 2200, Copenhagen, Denmark [3]Center for the study of Obesity, Polytechnic University of Marche, 60020, Ancona, Italy

[4] Ditte Neess and Vibeke Kruse contributed equally.

*Corresponding author. E-mail: s.mandrup@bmb.sdu.dk (S. Mandrup).

**Corresponding author. E-mail: nils.f@bmb.sdu.dk (N.J. Færgeman).

Received September 17, 2020 • Revision received December 3, 2020 • Accepted December 10, 2020 • Available online 18 December 2020

https://doi.org/10.1016/j.molmet.2020.101144

ACER1 [7]. Similarly, we previously showed that acyl-CoA-binding protein (ACBP) not only serves key functions in lipid metabolism in mammals [8,9], but also that ACBP in keratinocytes is required to maintain an intact epidermal barrier and normal fur to prevent alopecia [10]. Skin-specific loss of ACBP also increases lipolysis in white adipose tissue (WAT) and changes hepatic lipid metabolism [11], indicating that lipid metabolism in the skin affects systemic metabolism. Intriguingly, the effects on lipid metabolism in adipose and liver tissues can be rescued by applying an artificial barrier to the skin of ACBP$^{-/-}$ mice [11], indicating that the epidermal barrier function per se rather than lipid-derived signaling molecules lead to system-wide metabolic effects.

These findings prompted us to investigate how impairment of the epidermal barrier function affects whole-body energy metabolism. We show that mice with constitutive knockout of ACBP (ACBP$^{-/-}$) and mice with keratinocyte-specific knockout of ACBP (K14-ACBP$^{-/-}$) exhibited increased energy expenditure, browning of white adipose tissue, and resistance to high-fat diet-induced obesity. Importantly, we also demonstrate that these systemic effects on energy metabolism are recapitulated in flaky tail mice (*ma/ma Flg*$^{ft/ft}$), a widely used model of human atopic dermatitis, collectively showing that a compromised epidermal barrier leads to major effects on systemic energy homeostasis.

2. METHODS

2.1. Animal experiments

Mice with constitutive- and conditional targeting of the *Acbp* gene were previously described [11,12]. The *ma/ma Flg*$^{ft/ft}$ mice used in this study were obtained from the Jackson Laboratories and back-crossed to wild-type C57BL/6J mice for at least 10 generations to obtain a congenic background. Unless stated otherwise, male mice were group housed on a 12-h light/dark cycle and given ad libitum access to water and chow food (Altromin 1324). For HFD feeding, the mice were housed individually and D12492 (Research Diets) was administered ad libitum. Housing at either a thermoneutral temperature (30 °C) or cold exposure (4 °C) was performed with individually housed mice for 72 h. Propranolol injections (20 mg/kg) were administered by I.P. injection once every day for 5 days in the mice housed at 22 °C. All animal of the experiments and transgenic mice breeding were approved by the Danish Animal Experiment Inspectorate.

2.2. Real-time PCR

Tissue was homogenized in TRI reagent (Sigma—Aldrich) and RNA was isolated according to the manufacturer's protocol. The RNA concentration and quality were evaluated using a NanoDrop 1000 spectrophotometer and gel electrophoresis. RNA was treated with DNase I (Invitrogen), and cDNA was prepared as previously described [12]. The mRNA expression levels were determined by real-time PCR and normalized to the *Tfiib* expression. All of the quantitative PCR analyses were conducted on LightCycler 480 Multiwell Plates 384. The primers used are listed in Table S1.

2.3. Western blotting analysis

Protein extracts were prepared and analyzed as previously described [12]. The primary antibodies used were anti-UCP1 (1:1000) (ab10983, Abcam) and anti-b-actin (1:1000) (A5441, Sigma—Aldrich). B-actin was used as a loading control. The secondary antibody was horseradish peroxidase-conjugated goat anti-rabbit or goat anti-mouse IgG (1:7500) (Promega).

2.4. Cold exposure

The mice were individually caged and housed at 4 °C for 3 days with ad libitum access to chow food and water. The mice were sacrificed by anesthesia (25% hypnorm, 25% dormicum in sterile water, and 0.01 m/g mouse) followed by blood collection by heart puncture and transcardial perfusion with PBS or 4% PFA depending on the following experiments.

2.5. Sample preparation for microscopy

The mice were anesthetized and transcardially perfused with PBS followed by 4% PFA in 0.1 M of phosphate buffer at a pH of 7.4. The iWAT was dissected and fixed overnight at 4 °C. The tissues were subsequently stored in 0.1% PFA at 4 °C until processing. The tissues were dehydrated and paraffin embedded. De-waxed sections were stained with anti-UCP1 (ab10983, Abcam), which was detected with an VECTASTAIN ABC kit (Vector Laboratories).

2.6. Indirect calorimetry and activity monitoring

Indirect calorimetry was performed using a PhenoMaster Home Cage System (TSE Systems). The mice were allowed to acclimate to metabolic chambers for 3—5 days prior to the measurement. Gas exchanges and food intake were recorded every 5 min. All of the metabolic phenotyping data were analyzed by averaging data from 3 days of measurements. The activity of the ACBP$^{-/-}$ and K14-ACBP$^{-/-}$ mice was assessed using implanted telemetric activity-monitoring devices. To implant the telemetric activity-monitoring devices, the mice were anesthetized with isoflurane and kept on heated pads during the procedure. G2 E-Mitter Telemetry System devices (Starr Life Sciences) were surgically implanted subcutaneously above the shoulder blades and sutured into place. ER4000 Receivers were placed under the cages within TSE cabinets. The activity of the *ma/ma Flg*$^{ft/ft}$ mice was monitored using TSE PhenoMasterNG ActiMot3 infrared light beam sensor frames. Physical activity data were integrated into PhenoMaster software.

2.7. Statistical analysis

Unless otherwise noted, statistical analysis was performed using GraphPad Prism version 8.4.3. Statistical parameters, including the value of n, are noted in the figure legends. Unless otherwise noted, all of the data are presented as means ± SEM. The statistical significance level was set at $p < 0.05$. For gene expression data, an unpaired parametric Student's t test was used to compare gene expression levels between two genotypes. Repeated measures data were assessed with two-way ANOVA.

3. RESULTS

3.1. ACBP in keratinocytes is indispensable for normal systemic energy expenditure

We previously reported that ACBP serves key functions in lipid metabolism in mammals [8,9] and ACBP in keratinocytes is required to maintain an intact epidermal barrier and normal fur to prevent alopecia [10]. To examine how systemic energy homeostasis was affected in the ACBP knockout mice, we applied indirect calorimetry to evaluate their energy expenditure, respiratory exchange ratio (RER), locomotor activity, and food intake. At room temperature, the ACBP$^{-/-}$ mice exhibited significantly increased O_2 consumption, RER, and food intake compared with their wild-type littermates, whereas their body weight and locomotor activity remained similar (Figure 1 and Supplementary Figure 1A-C and 2). This indicated that their systemic energy expenditure increased and the ACBP$^{-/-}$ mice displayed a substrate

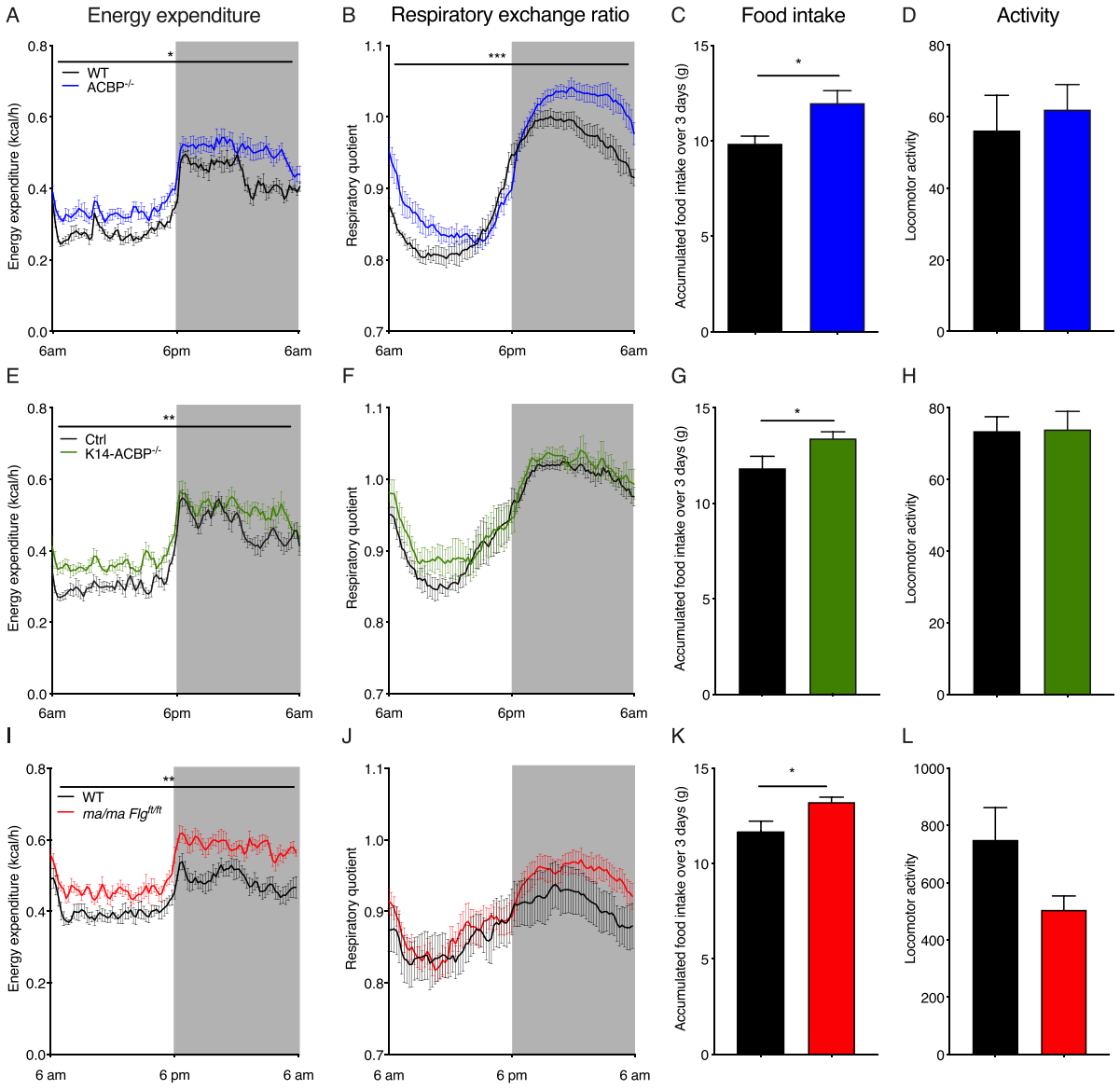

Figure 1: Impaired epidermal barrier leads to an increased metabolic rate at room temperature. (A) Energy expenditure at 22 °C of the wild-type (WT) and ACBP$^{-/-}$ mice housed in metabolic cages (n = 6 per group, average of 3 days, two-way ANOVA). (B) RQ at 22 °C of the WT and ACBP$^{-/-}$ mice housed in metabolic cages (n = 6 per group, average of 3 days, two-way ANOVA). (C) Food intake at 22 °C of the WT and ACBP$^{-/-}$ mice recorded over 3 days in metabolic cages (n = 6 per group, Student's t test). (D) Locomotor activity at 22 °C of the WT and ACBP$^{-/-}$ mice recorded over 3 days in metabolic cages (n = 6 per group, Student's t test). (E) Energy expenditure at 22 °C from the control and K14-ACBP$^{-/-}$ mice housed in metabolic cages (n = 6 per group, average of 3 days, two-way ANOVA). (F) RQ at 22 °C of the control and K14-ACBP$^{-/-}$ mice housed in metabolic cages (n = 6 per group, average of 3 days, two-way ANOVA). (G) Food intake at 22 °C of the control and K14-ACBP$^{-/-}$ mice recorded over 3 days in metabolic cages (n = 6 per group, Student's t test). (H) Locomotor activity at 22 °C of the WT and K14-ACBP$^{-/-}$ mice recorded over 3 days in metabolic cages (n = 6 per group, Student's t test). (I) Energy expenditure at 22 °C of the WT and *ma/ma Flg$^{ft/ft}$* mice housed in metabolic cages (n = 8 per group, average of 3 days, two-way ANOVA). (J) RQ at 22 °C of the WT and *ma/ma Flg$^{ft/ft}$* mice housed in metabolic cages (n = 8 per group, average of 3 days, two-way ANOVA). (K) Food intake at 22 °C of the WT and *ma/ma Flg$^{ft/ft}$* mice recorded over 3 days in metabolic cages (n = 8 per group, Student's t test). (L) Locomotor activity at 22 °C of the WT and *ma/ma Flg$^{ft/ft}$* mice recorded over 3 days in metabolic cages (n = 8 per group, Student's t test). Data are presented as the mean of individuals in each group ±SEM. *p < 0.05, **p < 0.01, and ***p < 0.001.

preference favoring carbohydrates. Similar to the full-body knockout, the K14-ACBP$^{-/-}$ mice displayed increased oxygen consumption and food intake compared with their control littermates (Figure 1 and Supplementary Figure 1), indicating that the increased energy expenditure was linked to the function of ACBP in keratinocytes. Notably, the RER of the K14-ACBP$^{-/-}$ mice remained comparable to that of the control mice (Figure 1), showing that the increased RER of the ACBP$^{-/-}$ mice was due to the absence of ACBP in cell types other than keratinocytes. Similar to the ACBP$^{-/-}$ mice, we did not observe changes in the locomotor activity or body weight of the K14-ACBP$^{-/-}$ mice compared with the control mice (Figure 1). Taken together, these results showed that loss of ACBP expression in keratinocytes led to an increase in whole-body energy expenditure.

Since trans-epidermal water loss (TEWL) significantly increased in both the full-body ACBP$^{-/-}$ and K14-ACBP$^{-/-}$ mice [13], we speculated that the increased energy expenditure in these mouse models was

caused by the impaired epidermal barrier. To investigate this, we used another mouse model, the flaky tail mice (*ma/ma Flg*$^{ft/ft}$), which carry a frameshift mutation in the filaggrin gene and a mutation in the *Tmem79* gene (*matted, ma*). These mice display increased trans-epidermal water loss, develop alopecia, and are widely used as a model of human atopic dermatitis associated with FLG mutations [14,15]. Interestingly, similar to the ACBP$^{-/-}$ mice, the *ma/ma Flg*$^{ft/ft}$ mice exhibited a significantly increased energy expenditure and food intake, while the RER remained similar to the control mice (Figure 1). Taken together, these findings indicated that defects in the epidermal barrier have a major impact on systemic energy metabolism.

3.2. A compromised epidermal barrier induces browning of inguinal white adipose tissue

It is well established that prolonged exposure to cold activates thermogenic responses in both humans and rodents, leading to the activation of BAT and browning of white adipose tissue (WAT) [16,17]. To investigate whether the compromised epidermal barrier induces a thermogenic response, we isolated BAT and iWAT from the ACBP$^{-/-}$, K14-ACBP$^{-/-}$, *ma/ma Flg*$^{ft/ft}$, and control littermates housed at room temperature and determined the expression of thermogenic genes. Notably, there was no significant change in the expression of thermogenic markers including uncoupling protein 1 (UCP1) in BAT in all of the mouse models with compromised epidermal barriers (Supplementary Figure 3 and 4). Interestingly, however, there was a modest but significant induction of thermogenic genes, including UCP1, iodothyronine deiodinase 2 (DIO2), and cell death-inducing DNA fragmentation factor-like effector A (CIDEA) in iWAT from the ACBP$^{-/-}$, K14-ACBP$^{-/-}$, and *ma/ma Flg*$^{ft/ft}$ mice (Figure 2A–C). Consistent with this, the number of multilocular adipocytes in iWAT from the ACBP$^{-/-}$, K14-ACBP$^{-/-}$, and *ma/ma Flg*$^{ft/ft}$ mice increased compared with iWAT from their WT littermates (Figure 2E–F). Furthermore, when the mice were exposed to 4 °C for three days, the induction of UCP1 in their iWAT markedly increased in all of the mouse models with compromised barrier compared with their control littermates (Figure 2D–F). These observations indicated that compromised epidermal barriers led to an increased thermogenic response in iWAT at 22 °C and 4 °C.

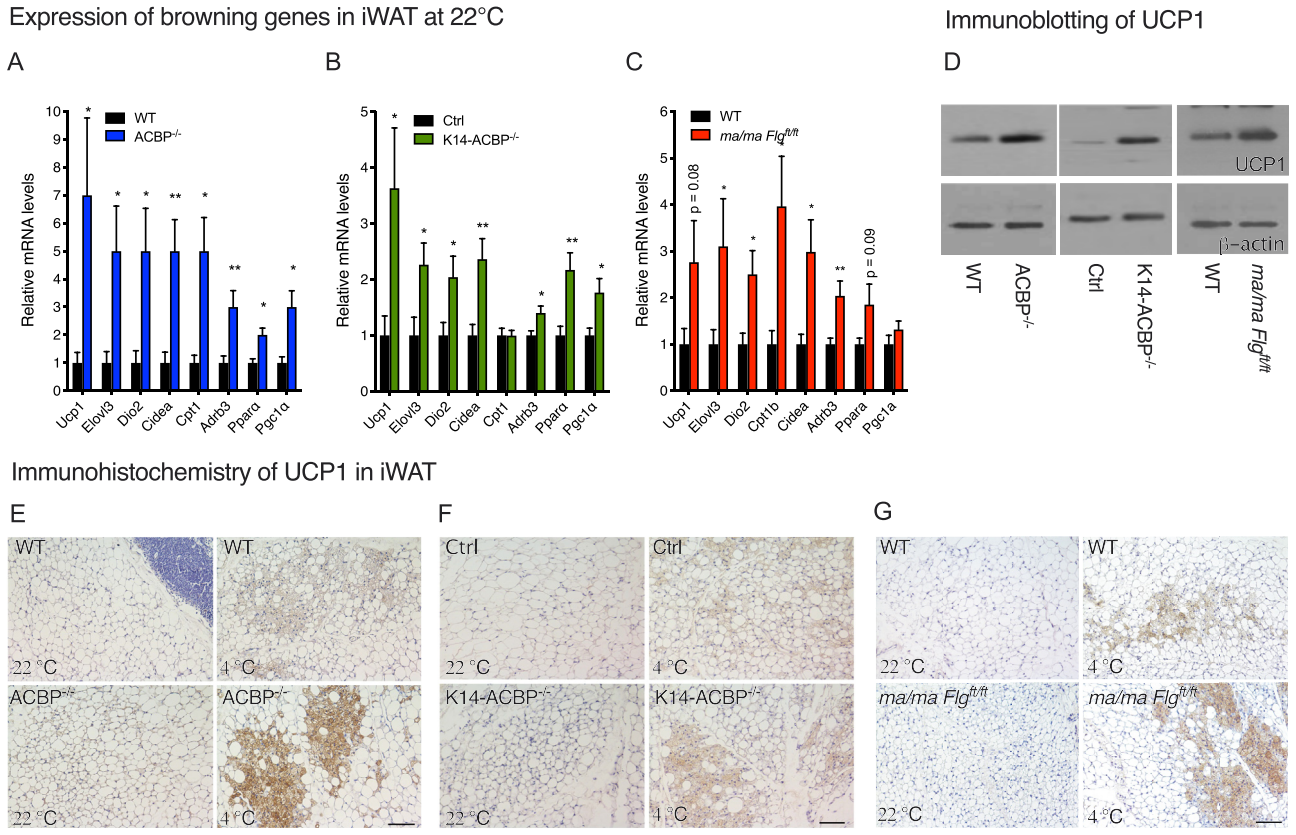

Figure 2: Disruption of ACBP in the skin induces browning of white adipose tissue. (A) mRNA levels of *Ucp1*, *Elovl3*, *Dio2*, *Cidea*, *Cpt1*, *Adrb3*, *Ppara*, and *Pgc1a* in iWAT of the WT and ACBP$^{-/-}$ mice housed at 22 °C (n = 12 per group, Student's t test). Data are presented as the mean of individuals in each group ±SEM. *p < 0.05 and **p < 0 .01. (B) mRNA levels of *Ucp1*, *Elovl3*, *Dio2*, *Cidea*, *Cpt1*, *Adrb3*, *Ppara*, and *Pgc1a* in iWAT of the control and K14-ACBP$^{-/-}$ mice housed at 22 °C (n = 12 per group, Student's t test). Data are presented as the mean of individuals in each group ±SEM. *p < 0.05 and **p < 0.01. (C) mRNA levels of *Ucp1*, *Elovl3*, *Dio2*, *Cidea*, *Cpt1*, *Adrb3*, *Ppara*, and *Pgc1a* in iWAT of the wild-type and *ma/ma Flg*$^{ft/ft}$ mice housed at 22 °C (n = 12 per group, Student's t test). Data are presented as the mean of individuals in each group ±SEM. *p < 0.05 and **p < 0.01. (D) UCP1 expression determined by Western blotting of iWAT from the wild-type, ACBP$^{-/-}$, K14-ACBP$^{-/-}$, and *ma/ma Flg*$^{ft/ft}$ mice housed at 4 °C for 3 days. Extracts from iWAT from four individual mice were pooled, analyzed by Western blotting, and probed for UCP1 (upper panel) and β-actin (lower panel). (E) Representative UCP1 immunostaining of iWAT from the control (upper) and ACBP$^{-/-}$ mice (lower) housed at 22 °C or 4 °C for 3 days at 10x magnification. Scale bars are 100 μm and each image represents 3 individuals. (F) Representative UCP1 immunostaining of iWAT from the control (upper) and K14-ACBP$^{-/-}$ mice (lower) housed at 22 °C or 4 °C for 3 days at 10x magnification. Scale bars are 100 μm and each image represents 3 individuals. (G) Representative UCP1 immunostaining of iWAT from the control (upper) and *ma/ma Flg*$^{ft/ft}$ mice (lower) housed at 22 °C or 4 °C for 3 days at 10x magnification. Scale bars are 100 μm and each image represents 3 individuals.

3.3. Housing at thermoneutrality rescues systemic energy expenditure and browning of iWAT

The results indicated that the increased energy expenditure in the mice with compromised epidermal barriers could have been due to increased thermogenic activity induced by the increased heat loss. To further investigate this, we housed the ACBP$^{-/-}$, K14-ACBP$^{-/-}$, and *ma/ma Flg*$^{ft/ft}$ mice and their control littermates in metabolic cages at 30 °C. Interestingly, thermoneutrality completely reversed the increased energy expenditure and O_2 consumption observed in the ACBP$^{-/-}$ and K14-ACBP$^{-/-}$ mice at 22 °C (Figure 3), whereas energy expenditure and O_2 consumption in the *ma/ma Flg*$^{ft/ft}$ mice were not fully rescued at 30 °C. Furthermore, the increased food intake of the three epidermal barrier-deficient mouse strains also reversed when they were housed at 30 °C (Figure 3). Similarly, housing at thermoneutrality (30 °C) blunted the induction of browning genes observed at 22 °C in the iWAT of the ACBP$^{-/-}$, K14-ACBP$^{-/-}$, and *ma/ma Flg*$^{ft/ft}$

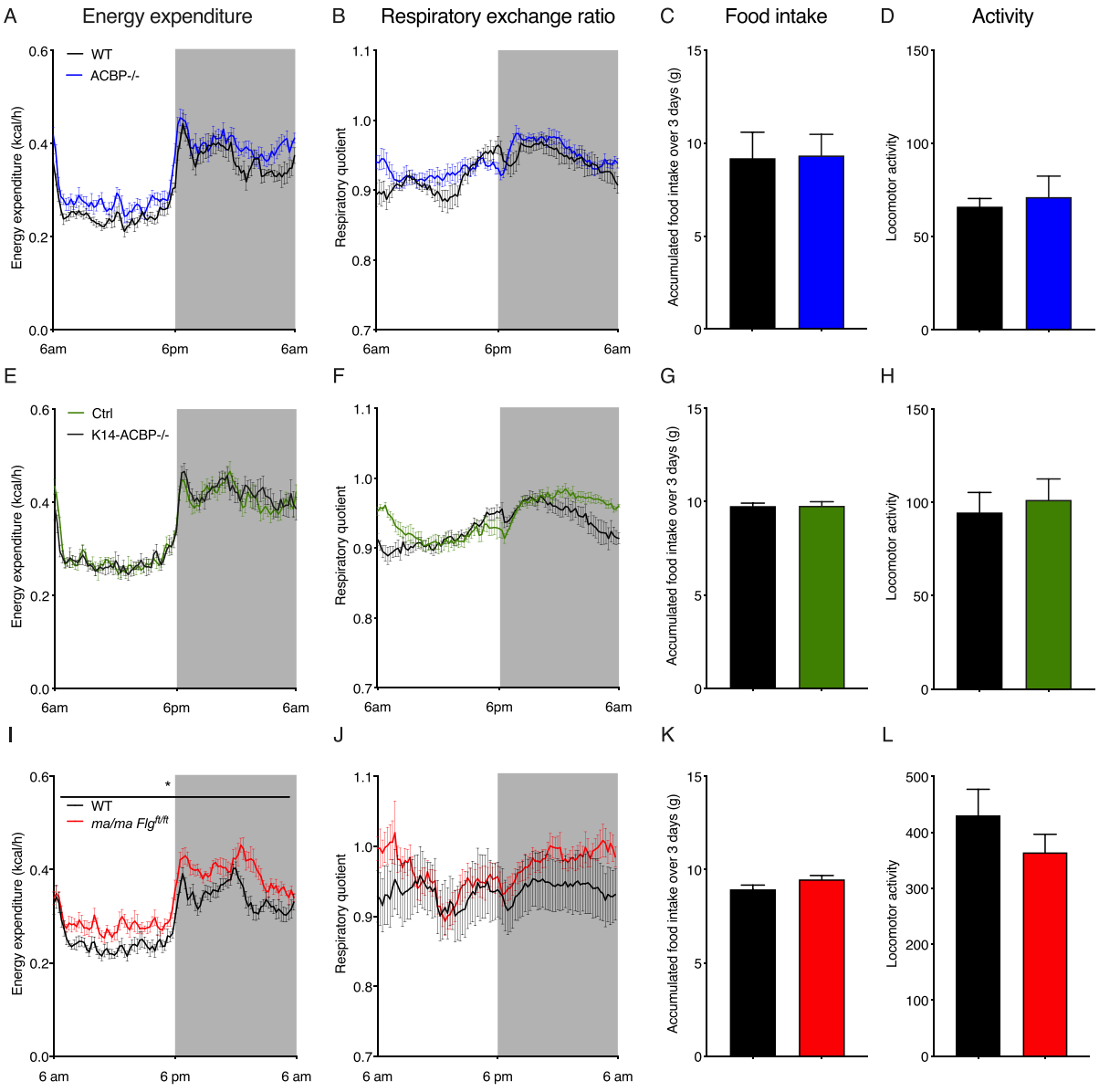

Figure 3: Thermoneutrality rescues energy homeostasis in mice with compromised epidermal barriers. (A) Energy expenditure at 30 °C of the WT and ACBP$^{-/-}$ mice housed in metabolic cages (n = 6 per group, average of 3 days, two-way ANOVA). (B) RQ at 30 °C of the WT and ACBP$^{-/-}$ mice housed in metabolic cages (n = 6 per group, average of 3 days, two-way ANOVA). (C) Food intake at 30 °C of the WT and ACBP$^{-/-}$ mice recorded over 3 days in metabolic cages (n = 6 per group, Student's t test). (D) Locomotor activity at 30 °C of the WT and ACBP$^{-/-}$ mice recorded over 3 days in metabolic cages (n = 6 per group, Student's t test). (E) Energy expenditure at 30 °C of the control and K14-ACBP$^{-/-}$ mice housed in metabolic cages (n = 6 per group, average of 3 days, two-way ANOVA). (F) RQ at 30 °C of the control and K14-ACBP$^{-/-}$ mice housed in metabolic cages (n = 6 per group, average of 3 days, two-way ANOVA). (G) Food intake at 30 °C of the control and K14-ACBP$^{-/-}$ mice recorded over 3 days in metabolic cages (n = 6 per group, Student's t test). (H) Locomotor activity at 30 °C of the WT and K14-ACBP$^{-/-}$ mice recorded over 3 days in metabolic cages (n = 6 per group, Student's t test). (I) Energy expenditure at 30 °C of the WT and *ma/ma Flg*$^{ft/ft}$ mice housed in metabolic cages (n = 8 per group, average of 3 days, two-way ANOVA). (J) RQ at 30 °C of the WT and *ma/ma Flg*$^{ft/ft}$ mice housed in metabolic cages (n = 8 per group, average of 3 days, two-way ANOVA). (K) Food intake at 30 °C of the WT and *ma/ma Flg*$^{ft/ft}$ mice recorded over 3 days in metabolic cages (n = 8 per group, Student's t test). (L) Locomotor activity at 30 °C of the WT and *ma/ma Flg*$^{ft/ft}$ mice recorded over 3 days in metabolic cages (n = 8 per group, Student's t test). Data are presented as the mean of individuals in each group ±SEM. *p < 0.05, **p < 0.01, and ***p < 0.001.

mice compared with their control littermates (Figure 4A–C). These results indicated that the increased thermogenic gene expression in the mice with compromised epidermal barriers was caused by heat loss and increased cold perception and that increased thermogenic activity led to increased energy expenditure and elevated food intake. The catecholamines adrenaline and noradrenaline control browning and fat cell metabolism mainly through activation of β-adrenoceptors on adipocytes [18]. Since there is little to no sympathetic activity in adipose tissue at thermoneutrality [19], we examined whether the increased browning of iWAT in the mice with compromised epidermal barriers at room temperature depended on β-adrenoceptor signaling. Hence, we injected the mice with propranolol for five days to block β-adrenergic signaling and subsequently examined browning of their iWAT and food intake. The results showed that propranolol injections blunted the induction of browning genes in the ACBP$^{-/-}$, K14-ACBP mice$^{-/-}$, and *ma/ma Flg$^{ft/ft}$* mice (Figure 4D–F), indicating that the thermogenic response was mediated via β-adrenergic signaling. Moreover, the propranolol injections also reversed the increased food intake in the mouse strains at 22 °C (Supplementary Figure 5). Collectively, our findings showed that compromised barrier function increases thermogenesis and β-adrenergic-dependent browning of the iWAT, leading to an overall increase in energy expenditure.

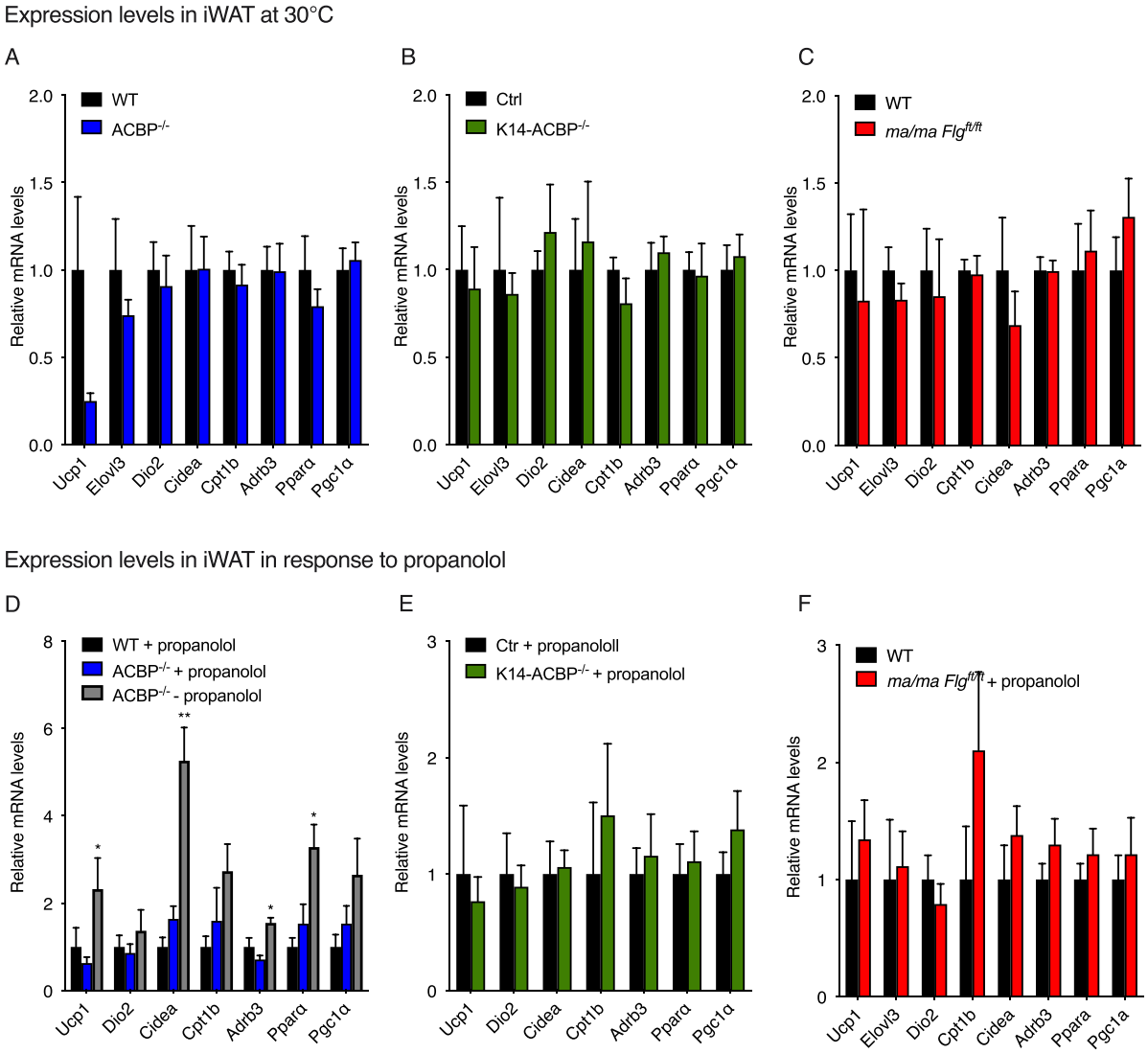

Figure 4: Blocking β-adrenergic signaling prevents browning of inguinal white adipose tissue in ACBP knockout mice. (A) mRNA levels of *Ucp1*, *Elovl3*, *Dio2*, *Cidea*, *Cpt1*, *Adrb3*, *Ppara*, and *Pgc1a* in iWAT of the WT and ACBP$^{-/-}$ mice housed at 30 °C (n = 7–8 per group, Student's t test). Data are presented as the mean of individuals in each group ± SEM. (B) mRNA levels of *Ucp1*, *Elovl3*, *Dio2*, *Cidea*, *Cpt1*, *Adrb3*, *Ppara*, and *Pgc1a* in iWAT of the WT and K14-ACBP$^{-/-}$ mice housed at 30 °C (n = 7–8 per group, Student's t test). Data are presented as the mean of individuals in each group ± SEM. (C) mRNA levels of *Ucp1*, *Elovl3*, *Dio2*, *Cidea*, *Cpt1*, *Adrb3*, *Ppara*, and *Pgc1a* in iWAT of the WT and *ma/ma Flg$^{ft/ft}$* mice housed at 30 °C (n = 7–8 per group, Student's t test). Data are presented as the mean of individuals in each group ± SEM. (D) mRNA levels of *Ucp1*, *Dio2*, *Cidea*, *Cpt1*, *Adrb3*, *Ppara*, and *Pgc1a* in iWAT of the control or propranolol-injected WT and ACBP$^{-/-}$ mice housed at 22 °C (n = 5–9 per group, Student's t test). Data are presented as the mean of individuals in each group ±SEM. *p < 0.05 and **p < 0 .01 between the ACBP$^{-/-}$ mice ± propranolol. (E) mRNA levels of *Ucp1*, *Dio2*, *Cidea*, *Cpt1*, *Adrb3*, *Ppara*, and *Pgc1a* in iWAT of the control or propranolol-injected control and K14-ACBP$^{-/-}$ mice housed at 22 °C (n = 5–9 per group, Student's t test). Data are presented as the mean of individuals in each group ± SEM. (F) mRNA levels of *Ucp1*, *Dio2*, *Cidea*, *Cpt1*, *Adrb3*, *Ppara*, and *Pgc1a* in iWAT of the control or propranolol-injected wild-type and *ma/ma Flg$^{ft/ft}$* mice housed at 22 °C (n = 5–9 per group, Student's t test). Data are presented as the mean of individuals in each group ± SEM.

3.4. Impaired epidermal barrier affords resistance to diet-induced obesity and improves glucose tolerance

Since the mice with compromised epidermal barriers displayed elevated energy expenditure, we next investigated whether these mice might also be resistant to diet-induced obesity. Thus, we subjected the ACBP$^{-/-}$, K14-ACBP$^{-/-}$, and *ma/ma Flg$^{ft/ft}$* mice and their control littermates to a high-fat diet (HFD) or standard chow for 12 weeks. When fed a standard chow diet, all of the mouse models with compromised epidermal barriers gained weight similar to their control littermates, although they ate significantly more than their littermates (Figure 5A,B, D, E, G, and H). Interestingly, however, all of the barrier-compromised strains were completely resistant to HFD-induced obesity, although their food intake was comparable to that of the control mice (Figure 5).

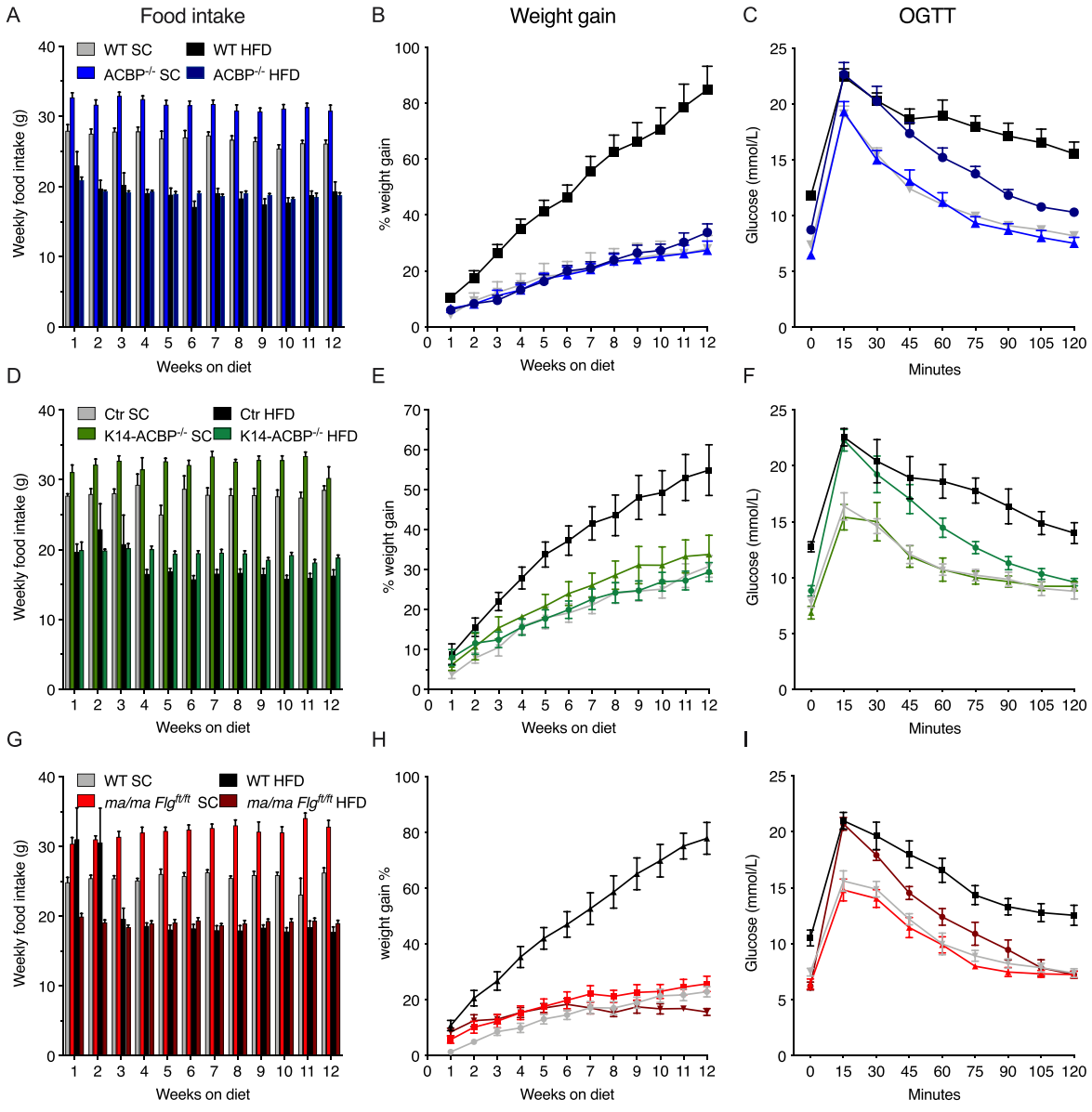

Figure 5: Impaired epidermal barriers protect mice against diet-induced obesity and glucose intolerance. (A) The WT and ACBP$^{-/-}$ mice were fed SC or HFD for 12 weeks. Food intake was determined every week for 12 weeks. (B) The WT and ACBP$^{-/-}$ mice were fed SC or HFD for 12 weeks. The mice were weighed every week and the percentage weight gain was plotted. Two-way ANOVA with multiple comparisons was applied. (C) The WT and ACBP$^{-/-}$ mice were fed SC or HFD for 12 weeks. Fasting blood glucose was determined prior to administration of 1.5 g/kg of glucose to each mouse by oral gavage and blood glucose was determined every 15 min for a period of 2 h. (D) The control and K14-ACBP$^{-/-}$ mice were fed SC or HFD for 12 weeks. Food intake was determined every week for 12 weeks. (E) The control and K14-ACBP$^{-/-}$ mice were fed SC or HFD for 12 weeks. The mice were weighed every week and the percentage weight gain was plotted. Two-way ANOVA with multiple comparisons was applied. (F) The control and K14-ACBP$^{-/-}$ mice were fed SC or HFD for 12 weeks. Fasting blood glucose was determined prior to administration of 1.5 g/kg of glucose to each mouse by oral gavage and blood glucose was determined every 15 min for a period of 2 h. (G) The WT and *ma/ma Flg$^{ft/ft}$* mice were fed SC or HFD for 12 weeks. Food intake was determined every week for 12 weeks. (H) The WT and *ma/ma Flg$^{ft/ft}$* mice were fed SC or HFD for 12 weeks. The mice were weighed every week and the percentage weight gain was plotted. Two-way ANOVA with multiple comparisons was applied. (I) The WT and *ma/ma Flg$^{ft/ft}$* mice were fed SC or HFD for 12 weeks. Fasting blood glucose was determined prior to administration of 1.5 g/kg of glucose to each mouse by oral gavage and blood glucose was determined every 15 min for a period of 2 h. All of the data are presented as the mean of individuals in each group ($n = 8$) $\pm$ SEM. *$p < 0.05$, **$p < 0.01$, and ***$p < 0.001$.

These observations prompted us to examine whether the mice with compromised epidermal barriers displayed increased glucose tolerance when fed a HFD. We therefore subjected the ACBP$^{-/-}$, K14-ACBP$^{-/-}$, and *ma/ma Flg$^{ft/ft}$* mice fed either a HFD or chow for 12 weeks to oral glucose tolerance tests (OGTTs) (Figure 5C,F, and I and Supplementary Figure 6). On a chow diet, their fasting glucose levels and glucose clearance was similar between the ACBP$^{-/-}$, K14-ACBP$^{-/-}$, and *ma/ma Flg$^{ft/ft}$* mice and their respective control littermates. However, on the HFD, all of the mouse models with compromised epidermal barriers were protected from an HFD-induced increase in fasting glucose concentrations and displayed increased glucose clearance relative to their control littermates (Figure 5C,F, and I). Notably, however, despite similar body weights, glucose clearance was lower in the HFD than the chow fed mutant mice, indicating that the HFD per se led to a compromised glucose tolerance independent of obesity. Notably, the ACBP$^{-/-}$ and K14-ACBP$^{-/-}$ mice on the HFD displayed plasma insulin levels comparable to that of the mice on the chow diet, whereas the *ma/ma Flg$^{ft/ft}$* mice on the HFD had significantly decreased plasma insulin levels compared with the control mice (Figure 6).

Plasma leptin levels are known to show a strong positive correlation with the amount of total body fat [20,21]. We found that the ACBP$^{-/-}$ and K14-ACBP$^{-/-}$ mice had plasma leptin concentrations comparable to that of the WT mice, whereas the *ma/ma Flg$^{ft/ft}$* mice had significantly decreased leptin levels. Consistent with the absence of HFD-induced obesity in the mice with compromised epidermal barriers, the plasma leptin levels in these mice were lower than in the control littermates when fed the HFD (Figure 6B,D, and F). Collectively, our data showed that despite similar food intake, the mice with compromised epidermal barriers were resistant to HFD-induced obesity and maintained normal fasting glucose and insulin levels on the HFD.

4. DISCUSSION

In this study, we showed that mice with impaired epidermal barrier function in the ACBP$^{-/-}$, K14-ACBP$^{-/-}$, and *ma/ma Flg$^{ft/ft}$* models displayed increased energy expenditure that appeared to be driven by increased thermogenesis. These mice were also completely protected from HFD-induced obesity and partially protected from the HFD-induced decrease in glucose clearance.

We previously showed that ablation of ACBP in the skin diminishes very long-chain fatty acid levels in the stratum corneum, which are required for epidermal barrier function [10]. As a consequence, the sebaceous and Harderian glands become hyperplastic and produce abnormally high levels of lipids, which are believed to be secreted to provide further insulation ([13] and our unpublished results). The present findings showed that the ACBP$^{-/-}$ and K14-ACBP$^{-/-}$ mice also upregulated their energy expenditure to defend their body temperature when housed at room temperature. The increased energy expenditure of the ACBP$^{-/-}$ and K14-ACBP$^{-/-}$ mice was so profound that they were resistant to diet-induced obesity and the diabetogenic effects of a high-fat diet. This is contrary the effect of ablation of ACBP in astrocytes in the arcuate nucleus, which has been shown to promote diet-induced hyperphagia and obesity in mice [22]. Thus, systemic effects resulting from loss of ACBP in keratinocytes appeared to override the effects of ACBP in astrocytes to control energy balance and its anorectic effects.

Interestingly, we found that the ACBP$^{-/-}$ mice displayed an increased RER compared with the WT mice, whereas the RER of the K14-ACBP$^{-/-}$ and *ma/ma Flg$^{ft/ft}$* mice was similar to that of the control mice, indicating that the rise in the RER was not caused by the increased energy metabolism. Instead, the increase in the RER indicated that a lack of ACBP in cell types other than keratinocytes led to an increase in the ratio of carbohydrates to fatty acid oxidation. This finding was in line with the observation that ACBP is required to sustain fatty acid oxidation in glioma cells [23] and human lung cancer cells [24] and is able to mediate transport of long-chain acyl-CoA esters to mitochondria in vitro [25].

Other mouse models with impaired synthesis of epidermal lipids support the notion that epidermal lipid metabolism plays a major role in epidermal barrier function. For instance, loss of elongation of very long-chain fatty acid (ELOVL3), diacylglycerol O-acyltransferase 1 (DGAT1), stearoyl-CoA desaturase (SCD1), or alkaline ceramide (ACER1) also impair synthesis of epidermal barrier lipids in mice, enhance evaporative cooling, increase whole-body energy expenditure, and render the mice resistant to diet-induced obesity [4,5,7,26,27]. To substantiate the epidermal barrier's role in systemic energy metabolism, we also showed that the mice with functional loss of filaggrin and Tmem79, which are not involved in lipid metabolism per se [28], shared several phenotypic characteristics of the ACBP$^{-/-}$ mice including increased TEWL, tousled fur, alopecia, and enlarged Harderian glands ([14,15] and our unpublished results) and exhibited elevated energy expenditure. Therefore, in addition to epidermal lipid metabolism, loss of structural entities such as filaggrin is also required to maintain systemic energy metabolism. However, housing the mice at 30 °C only reversed the increased energy expenditure and VO_2 in the ACBP$^{-/-}$ and K14-ACBP$^{-/-}$ mice but not in the *ma/ma Flg$^{ft/ft}$* mice. We speculate that the *ma/ma Flg$^{ft/ft}$* mice might have had a higher thermoneutral set point, which may have been due to a more adverse skin phenotype than the ACBP$^{-/-}$ and K14-ACBP$^{-/-}$ mice, making the *ma/ma Flg$^{ft/ft}$* mice moderately cold challenged even at 30 °C.

Our observations are in line with recent studies showing that a compromised epidermal barrier augments evaporative cooling at the body surface, which further enhances energy expenditure that accounts for a significant proportion of total systemic energy metabolism in mice [29]. Moreover, shaving wild-type mice increases their metabolic rate at room temperatures (approximately 22 °C) by approximately 50% due to increased heat loss [30], which nearly corresponds to transferring an unshaved mouse from 20 °C to 10 °C [31]. Nedergaard and Cannon stated that at 20 °C, the extra metabolism required to counteract the extra heat loss due to shaving is nearly 3 times higher than that of an unshaved mouse. Additionally, genetically nude Balb/c mice have a metabolic rate that is almost 2 times higher than that of normal Balb/c mice [30]. Thus, impaired insulation caused by changes in the quality of the fur and hair resembles exposure to colder ambient temperatures.

Cold exposure leads to a profound increase in whole-body energy expenditure in small rodents, and activating non-shivering thermogenesis in brown adipose tissue (BAT) plays a key role in defending body temperature during prolonged cold exposure [32]. In this study, the expression of UCP1 and other thermogenic markers neither increased in the BAT of the full-body ACBP$^{-/-}$ and skin-specific K14-ACBP$^{-/-}$ mice, nor in the *ma/ma Flg$^{ft/ft}$* mice at 22 °C or at 30 °C. However, we consider it likely that increased thermogenic activity in BAT induced by non-transcriptional mechanisms may also have played a role in the increased energy expenditure in the mice with compromised epidermal barriers. Analysis of iWAT demonstrated modest browning at room temperature and a more pronounced browning at 4 °C in the three mouse models with compromised epidermal barriers compared with their littermate controls. Further analyses indicated that

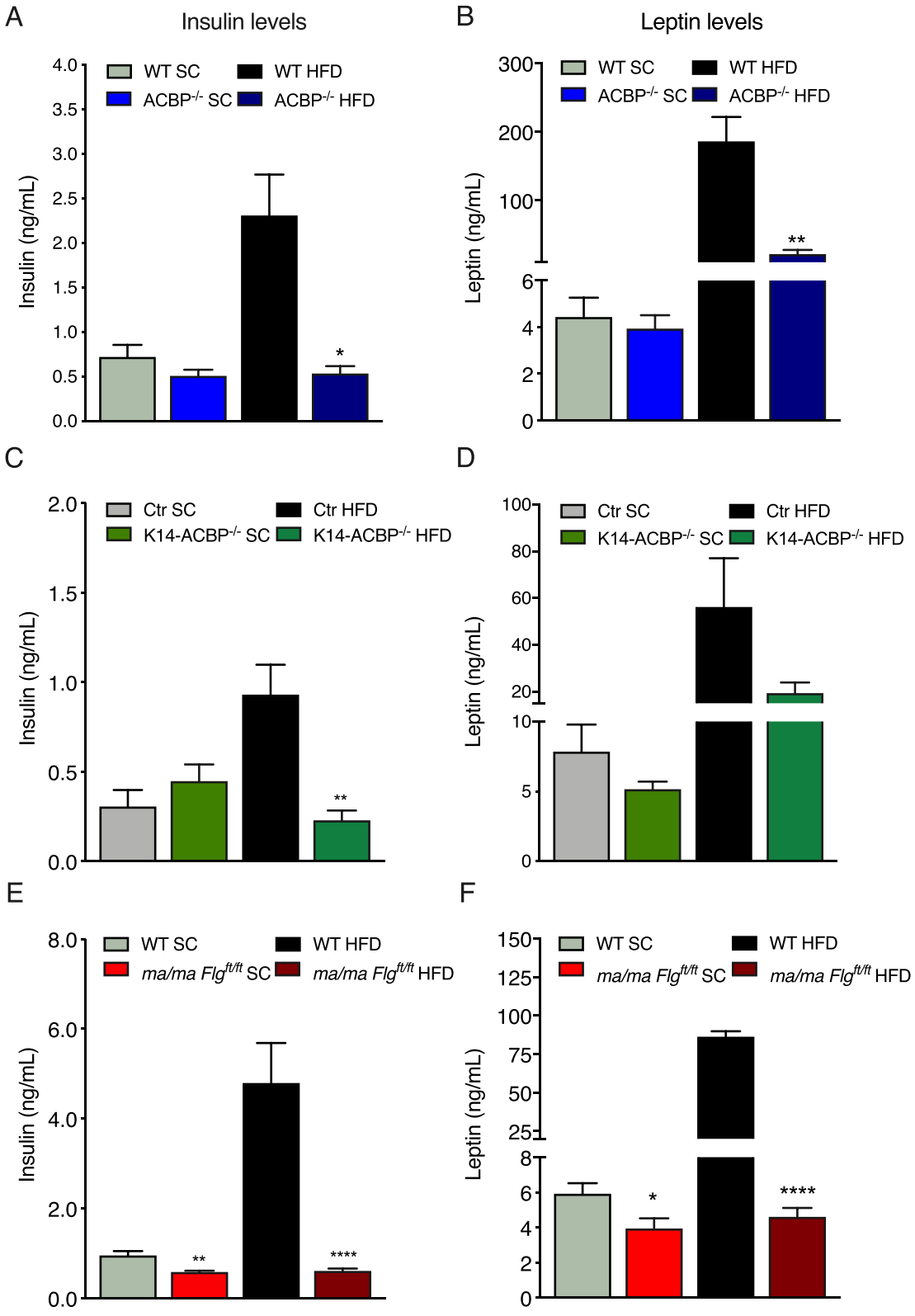

Figure 6: Impaired epidermal barrier protects mice against diet-induced hyperinsulinemia. (A) Plasma insulin levels in the WT and ACBP$^{-/-}$ mice fed either SC or HFD for 12 weeks. (B) Plasma leptin levels in the WT and ACBP$^{-/-}$ mice fed either SC or HFD for 12 weeks. (C) Plasma insulin levels in the control and K14-ACBP$^{-/-}$ mice fed either SC or HFD for 12 weeks. (D) Plasma leptin levels in the control and K14-ACBP$^{-/-}$ mice fed either SC or HFD for 12 weeks. (E) Plasma insulin levels in the WT and *ma/ma Flg*$^{ft/ft}$ mice fed either SC or HFD for 12 weeks. (F) Plasma leptin levels in the WT and *ma/ma Flg*$^{ft/ft}$ mice fed either SC or HFD for 12 weeks. All of the data are presented as the mean of individuals in each group ($n = 8$) $\pm$ SEM. *$p < 0.05$, **$p < 0.01$, and ***$p < 0.001$.

β-adrenergic signals are likely to play a major role in browning of iWAT, since blocking of β-adrenergic signaling by propranolol injections and housing at thermoneutrality completely alleviated browning of iWAT and normalized food intake. In line with this observation, it was recently demonstrated that a β3-adrenergic receptor agonist not only improves oral glucose tolerance and insulin sensitivity, but also stimulates browning of subcutaneous WAT in obese humans [33]. At present, we cannot exclude that thermogenic reprogramming could occur in BAT when mice with compromised epidermal barriers are housed at 4 °C. Such studies represent a novel avenue that will be pursued in the future.

The central nervous system regulates body temperature homeostasis via neural and hormonal cues at multiple levels. In rodents and humans, the skin, viscera, and central nervous system (CNS) provide temperature information directly or indirectly to the thermoregulatory center residing in the preoptic area of the hypothalamus [34]. This area is believed to integrate and compute temperature information and respond by signaling either directly or via other parts of the hypothalamus to multiple effector organs. Among the best-described pathways in thermoregulation is the neuronal modulation of non-shivering thermogenesis. Primary sensory neurons in the skin sense changes in ambient temperature via cold receptors, for example, TRPM8 in the skin [35]. These receptors signal to the preoptic area in the hypothalamus, which signals to sympathetic preganglionic neurons in the spinal cord that modulate norepinephrine release from sympathetic neurons innervating adipose tissues [34,36]. BAT thermogenesis is triggered by the release of norepinephrine, stimulating β3-adrenergic receptors that initiate a cascade of intracellular events resulting in activation of lipolysis, transcriptional and post-translational activation of UCP-1 and subsequently UCP1-mediated thermogenesis [37]. Intriguingly, sympathetic activation by β3-adrenergic receptor agonists or cold stress not only activates thermogenesis in BAT, but also causes the development of brown-like adipocytes in various white fat depots in wild-type mice [38]. We therefore speculate that changes in epidermal barrier functions augment activation and signaling through TRPM8, inducing thermogenic responses in white adipose tissue. We cannot entirely exclude that keratinocytes or other cells residing in the skin could possibly secrete a hitherto unknown factor mediating the activation of thermogenic programs in adipose tissues. However, we consider this unlikely as housing the mice at 30 °C and blocking β-adrenergic signaling blunted increased energy expenditure, O_2 consumption, and expression of browning genes in their iWAT.

To what extent the epidermal barrier contributes to regulating systemic energy metabolism in humans is not fully resolved. Not only is the skin's structure and morphology different between mice and humans, the surface-to-volume ratio is much greater in small rodents than humans and the adipose tissue is far less thermogenic in humans compared with rodents. Nevertheless, it is interesting to note that humans with burn injuries or children with ichthyosis exhibit not only increased trans-epidermal barrier disruption, but also elevated resting energy expenditure [39–41]. We showed that loss of ACBP in keratinocytes and the ensuing impairment of epidermal barrier function led to a profound increase in energy metabolism, browning of white adipose tissue, and protection against HFD-induced obesity, phenotypes that were recapitulated in the *ma/ma Flg*$^{ft/ft}$ mice. Our results indicated that an increase in epidermal barrier permeability can enhance systemic energy expenditure and hence protect against an increased accumulation of calories and eventually metabolic diseases.

FUNDING

This work was supported by the Independent Research Fund Denmark — Natural Sciences, The Novo Nordisk Foundation, the Lundbeck Foundation, the VILLUM Foundation through a grant to the VILLUM Center for Bioanalytical Sciences at the University of Southern Denmark, and NordForsk through a grant to the Nordic Center of Excellence MitoHealth.

AUTHOR CONTRIBUTIONS

D.N., A.-B. M., Z.G.-H., S.M., and N.J.F. conceived and designed the project. V.K, D.N, A.-B.M., M.R.W., J.V., P.M.M., J.R.B, R.P., G.C, I.S., T.M, and I.S. conducted the experiments. V.K., D.N., A.-B.M., Z.G.-H., M.R.W., J.V., P.M.M., R.P., T.M, G.C, I.S., S.M., and N.J.F. analyzed and interpreted the data. D.N. and N.J.F. wrote the original draft. D.N., A.-B.M., S.M., and N.J.F. wrote the final version.

ACKNOWLEDGMENTS

The skillful technical assistance of Ida Nørgaard Jensen is gratefully acknowledged.

CONFLICT OF INTEREST

None declared.

APPENDIX A. SUPPLEMENTARY DATA

Supplementary data to this article can be found online at https://doi.org/10.1016/j.molmet.2020.101144.

REFERENCES

[1] Feingold, K.R., Denda, M., 2012. Regulation of permeability barrier homeostasis. Clinical Dermatology 30(3):263–268.

[2] Kruse, V., Neess, D., Faergeman, N.J., 2017. The significance of epidermal lipid metabolism in whole-body physiology. Trends in Endocrinology and Metabolism 28(9):669–683.

[3] Natsuga, K., 2014. Epidermal barriers. Cold Spring Harbor PErspectives in Medicine 4(4):a018218.

[4] Sampath, H., Flowers, M.T., Liu, X., Paton, C.M., Sullivan, R., Chu, K., et al., 2009. Skin-specific deletion of steaCold Spring Harbor Perspectives in Medicineroyl-CoA desaturase-1 alters skin lipid composition and protects mice from high fat diet-induced obesity. Journal of Biological Chemistry 284(30): 19961–19973.

[5] Westerberg, R., Tvrdik, P., Unden, A.B., Mansson, J.E., Norlen, L., Jakobsson, A., et al., 2004. Role for ELOVL3 and fatty acid chain length in development of hair and skin function. Journal of Biological Chemistry 279(7):5621–5629.

[6] Zadravec, D., Brolinson, A., Fisher, R.M., Carneheim, C., Csikasz, R.I., Bertrand-Michel, J., et al., 2010. Ablation of the very-long-chain fatty acid elongase ELOVL3 in mice leads to constrained lipid storage and resistance to diet-induced obesity. The FASEB Journal 24(11):4366–4377.

[7] Liakath-Ali, K., Vancollie, V.E., Lelliott, C.J., Speak, A.O., Lafont, D., Protheroe, H.J., et al., 2016. Alkaline ceramidase 1 is essential for mammalian skin homeostasis and regulating whole-body energy expenditure. The Journal of Pathology 239(3):374–383.

[8] Neess, D., Bek, S., Engelsby, H., Gallego, S.F., Faergeman, N.J., 2015. Long-chain acyl-CoA esters in metabolism and signaling: role of acyl-CoA binding proteins. Progress in Lipid Research 59:1–25.

[9] Ferreira, N.S., Engelsby, H., Neess, D., Kelly, S.L., Volpert, G., Merrill, A.H., et al., 2017. Regulation of very-long acyl chain ceramide synthesis by acyl-CoA-binding protein. Journal of Biological Chemistry 292(18):7588–7597.

[10] Bloksgaard, M., Bek, S., Marcher, A.B., Neess, D., Brewer, J., Hannibal-Bach, H.K., et al., 2012. The acyl-CoA binding protein is required for normal epidermal barrier function in mice. The Journal of Lipid Research 53(10): 2162–2174.

[11] Neess, D., Bek, S., Bloksgaard, M., Marcher, A.B., Faergeman, N.J., Mandrup, S., 2013. Delayed hepatic adaptation to weaning in ACBP-/- mice is caused by disruption of the epidermal barrier. Cell Reports 5(5):1403–1412.

[12] Neess, D., Bloksgaard, M., Bek, S., Marcher, A.B., Elle, I.C., Helledie, T., et al., 2011. Disruption of the acyl-CoA-binding protein gene delays hepatic adaptation to metabolic changes at weaning. Journal of Biological Chemistry 286(5):3460–3472.

[13] Bek, S., Neess, D., Dixen, K., Bloksgaard, M., Marcher, A.B., Chemnitz, J., et al., 2015. Compromised epidermal barrier stimulates Harderian gland activity and hypertrophy in ACBP-/- mice. The Journal of Lipid Research 56(9):1738–1746.

[14] Sasaki, T., Shiohama, A., Kubo, A., Kawasaki, H., Ishida-Yamamoto, A., Yamada, T., et al., 2013. A homozygous nonsense mutation in the gene for Tmem79, a component for the lamellar granule secretory system, produces spontaneous eczema in an experimental model of atopic dermatitis. The Journal of Allergy and Clinical Immunology 132(5):1111–1120 e1114.

[15] Saunders, S.P., Goh, C.S., Brown, S.J., Palmer, C.N., Porter, R.M., Cole, C., et al., 2013. Tmem79/Matt is the matted mouse gene and is a predisposing gene for atopic dermatitis in human subjects. The Journal of Allergy and Clinical Immunology 132(5):1121–1129.

[16] Giordano, A., Smorlesi, A., Frontini, A., Barbatelli, G., Cinti, S., 2014. White, brown and pink adipocytes: the extraordinary plasticity of the adipose organ. European Journal of Endocrinology 170(5):R159–R171.

[17] Vosselman, M.J., van Marken Lichtenbelt, W.D., Schrauwen, P., 2013. Energy dissipation in brown adipose tissue: from mice to men. Molecular and Cellular Endocrinology 379(1–2):43–50.

[18] Patsouris, D., Qi, P., Abdullahi, A., Stanojcic, M., Chen, P., Parousis, A., et al., 2015. Burn induces browning of the subcutaneous white adipose tissue in mice and humans. Cell Reports 13(8):1538–1544.

[19] Cinti, S., 2005. The adipose organ. Prostaglandins Leukotrienes and Essential Fatty Acids 73(1):9–15.

[20] McGregor, G.P., Desaga, J.F., Ehlenz, K., Fischer, A., Heese, F., Hegele, A., et al., 1996. Radiommunological measurement of leptin in plasma of obese and diabetic human subjects. Endocrinology 137(4):1501–1504.

[21] Shimizu, H., Shimomura, Y., Hayashi, R., Ohtani, K., Sato, N., Futawatari, T., et al., 1997. Serum leptin concentration is associated with total body fat mass, but not abdominal fat distribution. International Journal of Obesity and Related Metabolic Disorders 21(7):536–541.

[22] Bouyakdan, K., Martin, H., Lienard, F., Budry, L., Taib, B., Rodaros, D., et al., 2019. The gliotransmitter ACBP controls feeding and energy homeostasis via the melanocortin system. Journal of Clinical Investigation 129(6):2417–2430.

[23] Duman, C., Yaqubi, K., Hoffmann, A., Acikgoz, A.A., Korshunov, A., Bendszus, M., et al., 2019. Acyl-CoA-binding protein drives glioblastoma tumorigenesis by sustaining fatty acid oxidation. Cell Metabolism 30(2):274–289 e275.

[24] Harris, F.T., Rahman, S.M., Hassanein, M., Qian, J., Hoeksema, M.D., Chen, H., et al., 2014. Acyl-coenzyme A-binding protein regulates Beta-oxidation required for growth and survival of non-small cell lung cancer. Cancer Prevention Research 7(7):748–757.

[25] Rasmussen, J.T., Faergeman, N.J., Kristiansen, K., Knudsen, J., 1994. Acyl-CoA-binding protein (ACBP) can mediate intermembrane acyl-CoA transport and donate acyl-CoA for beta-oxidation and glycerolipid synthesis. Biochemical Journal 299(Pt 1):165–170.

[26] Miyazaki, M., Kim, H.J., Man, W.C., Ntambi, J.M., 2001. Oleoyl-CoA is the major de novo product of stearoyl-CoA desaturase 1 gene isoform and substrate for the biosynthesis of the Harderian gland 1-alkyl-2,3-diacylglycerol. Journal of Biological Chemistry 276(42):39455–39461.

[27] Chen, H.C., Smith, S.J., Tow, B., Elias, P.M., Farese Jr., R.V., 2002. Leptin modulates the effects of acyl CoA:diacylglycerol acyltransferase deficiency on murine Fur and sebaceous glands. Journal of Clinical Investigation 109(2): 175–181.

[28] Mildner, M., Jin, J., Eckhart, L., Kezic, S., Gruber, F., Barresi, C., et al., 2010. Knockdown of filaggrin impairs diffusion barrier function and increases UV sensitivity in a human skin model. Journal of Investigative Dermatology 130(9): 2286–2294.

[29] Kasza, I., Adler, D., Nelson, D.W., Eric Yen, C.L., Dumas, S., Ntambi, J.M., et al., 2019. Evaporative cooling provides a major metabolic energy sink. Molecular Metabolism 27:47–61.

[30] Hirata, M., Suzuki, M., Ishii, R., Satow, R., Uchida, T., Kitazumi, T., et al., 2011. Genetic defect in phospholipase Cdelta1 protects mice from obesity by regulating thermogenesis and adipogenesis. Diabetes 60(7):1926–1937.

[31] Nedergaard, J., Cannon, B., 2014. The browning of white adipose tissue: some burning issues. Cell Metabolism 20(3):396–407.

[32] van der Lans, A.A., Hoeks, J., Brans, B., Vijgen, G.H., Visser, M.G., Vosselman, M.J., et al., 2013. Cold acclimation recruits human brown fat and increases nonshivering thermogenesis. Journal of Clinical Investigation 123(8): 3395–3403.

[33] Finlin, B.S., Memetimin, H., Zhu, B., Confides, A.L., Vekaria, H.J., El Khouli, R.H., et al., 2020. The beta3-adrenergic receptor agonist mirabegron improves glucose homeostasis in obese humans. Journal of Clinical Investigation 130(5):2319–2331.

[34] Morrison, S.F., 2016. Central neural control of thermoregulation and brown adipose tissue. Autonomic Neuroscience 196:14–24.

[35] McKemy, D.D., 2013. The molecular and cellular basis of cold sensation. ACS Chemical Neuroscience 4(2):238–247.

[36] Nakamura, K., Morrison, S.F., 2011. Central efferent pathways for cold-defensive and febrile shivering. Journal of Physiology 589(Pt 14):3641–3658.

[37] Morrison, S.F., Madden, C.J., Tupone, D., 2012. Central control of brown adipose tissue thermogenesis. Frontiers in Endocrinology 3(5).

[38] Jimenez, M., Barbatelli, G., Allevi, R., Cinti, S., Seydoux, J., Giacobino, J.P., et al., 2003. Beta 3-adrenoceptor knockout in C57BL/6J mice depresses the occurrence of brown adipocytes in white fat. European Journal of Biochemistry 270(4):699–705.

[39] Moskowitz, D.G., Fowler, A.J., Heyman, M.B., Cohen, S.P., Crumrine, D., Elias, P.M., et al., 2004. Pathophysiologic basis for growth failure in children with ichthyosis: an evaluation of cutaneous ultrastructure, epidermal permeability barrier function, and energy expenditure. The Journal of Pediatrics 145(1):82–92.

[40] Jeschke, M.G., Gauglitz, G.G., Kulp, G.A., Finnerty, C.C., Williams, F.N., Kraft, R., et al., 2011. Long-term persistance of the pathophysiologic response to severe burn injury. PloS One 6(7):e21245.

[41] Kraft, R., Kulp, G.A., Herndon, D.N., Emdad, F., Williams, F.N., Hawkins, H.K., et al., 2011. Is there a difference in clinical outcomes, inflammation, and hypermetabolism between scald and flame burn? Pediatric Critical Care Medicine 12(6):e275–e281.

